

# Effect of flow characteristics on the diffusion-limited current density in an electrodeposition cell

L. VANHÉE\*, J. C. MONNIER, R. WINAND<sup>†</sup>, M. STANISLAS<sup>§</sup>

IMFL-ONERA, 5 Bvd Paul Painlevé, 59000 Lille, France

Received 18 November 1992; revised 26 August 1993

The main parameters characterizing the effect of the turbulent flow of an electrolyte between two planar electrodes, one of which may be in motion, are demonstrated by means of numerical and experimental studies. The analysis is carried out for the case of zinc electrodeposition. A model is proposed, which takes into account the production of hydrogen, to represent the variation of the diffusion limited current density as a function of the flow characteristics and of the solution composition.

## 1. Introduction

The texture of an electrolytic deposit depends directly on the ratio of the current density used in the electrolytic process to the limiting current density,  $J/J_{\text{lim}}$  [1]. The motion of the electrolyte influences the diffusion-limited current density and therefore the texture of the deposit. To evaluate this influence, a numerical simulation of the flow and ion transport is necessary.

In most industrial and laboratory electroplating cells, the flow may be considered to be steady, also the fluid is supposed to have constant physical properties and chemical composition. The solution generally flows between two planar, parallel electrodes: the cathode, which receives the deposit, may be in motion, parallel to the anode. Under these conditions, the chemical and electrical phenomena occurring in the cell can be decoupled [2].

Once the flow characteristics have been determined, the transport of the depositing ions can be characterized by solving the corresponding transport equation. In the present study the particular case of the diffusion-limited current density, for a solution with a large excess of electrolyte, is adopted. It is also assumed that no chemical, electrical or crystallization mechanism limits the electroplating process. Migration can then be neglected [3]. Electroplating of metals like copper and zinc meets these requirements.

The analysis performed here has allowed modelling of the influence of the various flow and electrolyte characteristics on the diffusion-limited current density [4]. To obtain universal laws describing the electrodeposition phenomena, it is necessary to use local characteristic quantities of the flow in the

vicinity of the cathode instead of global quantities as, for example, the mean flow velocity and the hydraulic diameter of the cell.

The numerical results show that mass transfer at the cathode varies to a power 0.26 of the Schmidt number,  $Sc$ , when this number is close to 600. This is not in agreement with the laws that are generally found in the literature, for which the exponent is rather 1/3. As will be seen, the results presented here confirm the remarks made by Ibl [5], and an exponent of about 1/4 seems more likely.

To complete the numerical study, measurements were performed in a laboratory cell for electrodeposition of zinc at high current density. These measurements partially confirm the simulations and have allowed the proposed model to take into account the influence of the hydrogen production on the mass transfer at the wall (the presence of hydrogen is neglected in the numerical analysis). The comparison of numerical and experimental results has led to a complete model that describes the variations of the mass transfer coefficient,  $k$ , with the flow characteristics, the quantity of hydrogen released at the cathode, the composition of the solution and its temperature. The comparison of these results with measurements performed by other researchers [6] shows noticeable differences. These differences seem to stem mainly from the geometry of the cells used by these authors, and from the consequent approximations.

## 2. Numerical study

In most electroplating cells, the channel is rectangular and the distance between the electrodes is small compared to their width. Considering the order of magnitude of the electrolyte velocities, the flows are generally turbulent. Monnier [2] has shown that it is possible to simplify considerably the analysis of these flows by neglecting the effects of the chemical and electrical phenomena. The influence of some aspects

\* Beautor S. A., 02800 La Fère, France.

<sup>†</sup> ULB, Electrochemical Laboratory, av. F. Roosevelt 50, B 1050 Brussels, Belgium.

<sup>§</sup> Also LML, CNRS URA 1441, Cité Scientifique 59650 Villeneuve d'Ascq, France.

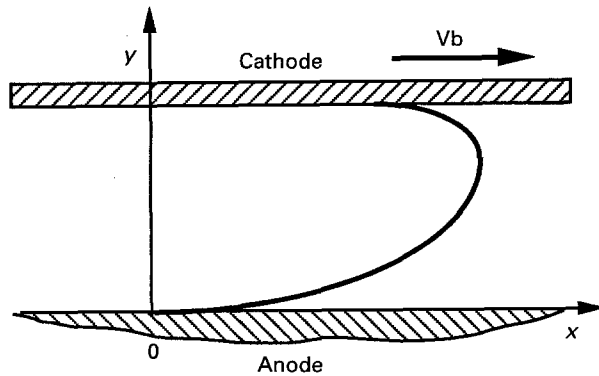


Fig. 1. Flow configuration in an electroplating cell.

of the cell geometry on the flow is also negligible. It may then be assumed that the flow is steady, turbulent, incompressible and that it is between two planar, parallel electrodes (Fig. 1). Generally, the electrodes are fixed in laboratory cells. The flow is then of Poiseuille type. In industrial electroplating lines, the cathode is in uniform motion, parallel to the anode. The flow in this case is of Couette-Poiseuille type. In the present study, both types of flow have been considered, to demonstrate the parameters which allow the transposition of results from laboratory to industrial cells.

For the dynamics of these two types of flows, the Reynolds equations reduces to the following form [2]:

$$\frac{d}{dy} \left( \nu \frac{dU}{dy} \right) - \frac{d}{dy} (\overline{uv}) = \frac{1}{\rho} \frac{d\hat{P}}{dx}$$

where  $U$  is the mean velocity in the  $x$  direction,  $-\rho\overline{uv}$  the Reynolds shear stress,  $\hat{P}$  the head pressure,  $\rho$  the density, and  $\nu$  the kinematic viscosity.

In the vicinity of a solid wall (presently the cathode), the variation of the flow properties is directly related to the friction velocity. This quantity can be predicted with a mixing length model which is sufficiently accurate for the purposes of the present study [2]. The equations to be solved are as follows:

$$\left. \begin{aligned} \frac{d}{dy} \left[ (\nu + \nu_t) \frac{dU}{dy} \right] &= \frac{1}{\rho} \frac{d\hat{P}}{dx} \\ \nu_t &= l^2 \left| \frac{dU}{dy} \right| \end{aligned} \right\} \quad (1)$$

in which  $l$  is the mixing length, and  $\nu_t$  the turbulent viscosity defined through the Boussinesq hypothesis:

$$-\overline{uv} = \nu_t \frac{dU}{dy}$$

No-slip boundary conditions are prescribed on each wall.

An industrial electrolytic solution contains an excess of acid to increase its conductivity. Due to this large acid concentration, transport by migration is negligible with respect to the other modes of ion transport. Since there is no production or

consumption in the solution of the species which deposits at the cathode, the transport equation for this depositing ion reduces to

$$U \frac{\partial C}{\partial x} = \frac{\partial}{\partial y} \left( D \frac{\partial C}{\partial y} \right) - \frac{\partial}{\partial y} (\overline{vc})$$

where  $C$  is the mean concentration and  $D$  the molecular diffusion coefficient of the species considered. Diffusion along the flow being negligible compared to diffusion normal to the wall, only one diffusion term appears in this equation [4].

Some hypothesis must be adopted at this stage concerning the term  $\overline{vc}$ . Investigations on heat transfer suggest a gradient transport model, analogous to that of Boussinesq:

$$-\overline{vc} = D_t \frac{\partial C}{\partial y}$$

where  $D_t$  is a turbulent diffusion coefficient, to be determined. The transport of matter and of momentum are analogous from a turbulent as well as a molecular point of view. Generally,

$$\nu = DSc \quad \nu_t = D_t Sc_t$$

where  $Sc$  is the molecular Schmidt number, whose order of magnitude is 600, and  $Sc_t$  the turbulent Schmidt number to be determined, and whose order of magnitude should be unity [3].

Finally, the transport equation for the depositing ion for turbulent flow is

$$U \frac{\partial C}{\partial x} = \frac{\partial}{\partial y} \left[ \left( \frac{\nu}{Sc} + \frac{\nu_t}{Sc_t} \right) \frac{\partial C}{\partial y} \right] \quad (2)$$

As can be seen from this equation, the mean velocity and eddy viscosity profiles are needed to determine  $C$ . For this purpose Equations 1 are solved, giving  $U$  and  $\nu_t$  on the entire height,  $h$ , of the channel (i.e. the distance between the electrodes). The obtained results are then used to solve Equation 2.

The present numerical study was concerned with the diffusion limited current density  $J_{lim}$ , which corresponds to a zero concentration of the ion to be deposited at the surface. This condition assumes that no chemical, electrical or crystallization process limits the electrodeposition process. Figure 2 gives a

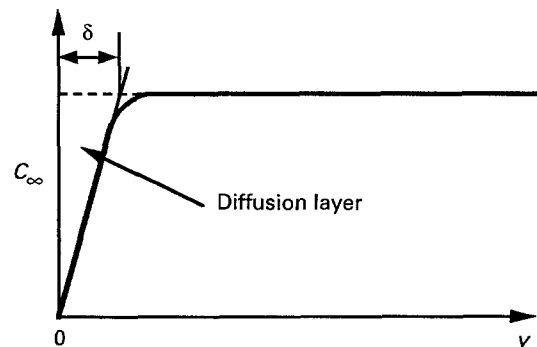


Fig. 2. Typical concentration profile in the case of diffusion limited current density.

typical concentration profile obtained in the case of the diffusion limited current density for a turbulent flow. It can be observed that the concentration is constant throughout the major part of the flow. The amount of ions deposited at the cathode is generally a very small part of the initial quantity of ions present in the solution. In this case, the concentration  $C_\infty$  far from the cathode is very close to that at the entrance of the cell. The concentration distribution varies only in the vicinity of the electrode, forming a diffusion layer whose characteristic thickness  $\delta$  is used in the definition of  $J_{lim}$ :

$$J_{lim} = \frac{zFDC_\infty}{\delta}, \quad \delta = \frac{C_\infty}{\left. \frac{\partial C}{\partial y} \right|_{y=0}} \quad (3)$$

where  $z$  is the charge number and  $F$  the Faraday constant.

The diffusion layer is generally very thin (of the order of a few micrometres). For this reason, and to save computer cost, the grid generated to solve Equation 2 has been limited to a domain extending to  $y_\infty = 1$  mm from the electrode. The conditions imposed on the boundaries of this domain are as follows:

$$\begin{aligned} x < 0, \quad \forall y & : C = C_\infty \\ x > 0, \quad y = y_\infty & : C = C_\infty \\ x > 0, \quad y = 0 & : C = 0 \end{aligned}$$

Equations 1 and 2 were solved by a finite-volume method, using a second order centred finite-difference discretization. The grid grows exponentially from the wall toward the centre of the channel, as well as from the origin of the diffusion layer in the flow direction. The grid independency of the results has been verified. For each flow the different parameters of the problem were then varied to study their influence.

The examination of the results reveals three different steps in the film evolution (Fig. 3). The incipient film is totally included in the viscous sublayer (step 1): it is very weakly affected by the flow turbulence and it thickens in the same way as it

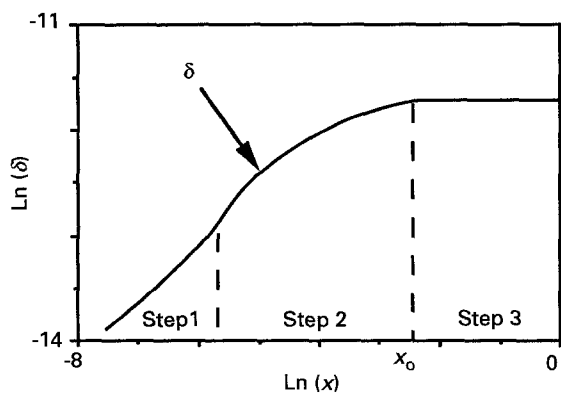


Fig. 3. Thickness  $\delta$  of the diffusion film as a function of the abscissa  $x$  along the cathode.

would in laminar flow. At step 2, the film becomes more and more influenced by turbulence. Finally, at  $x_0$ , the diffusion layer ceases to thicken (step 3). The concentration profile then remains unchanged. This steadiness is due to turbulent diffusion which balances the consumption of ions at the surface. It appears from the present results that, for this type of electrolyte, the diffusion and viscous films have thicknesses of the same order of magnitude. As  $J_{lim}$  is related to the diffusion film thickness through Equation 3 it is also constant. The texture of the deposit can thus be controlled in the region  $x > x_0$ . As a consequence, the length  $x_0$  is an important parameter which must be determined in order to know the distance beyond which the required texture conditions are obtained. It will also allow estimation of the influence of the establishment region on the diffusion limited current density measurements in laboratory cells.

Whether the flow is of Poiseuille (in a laboratory cell) or Couette–Poiseuille type (in an industrial cell), the following results are obtained from the numerical simulations for  $x > x_0$ :

$$\left. \begin{aligned} \frac{\delta u_\tau}{\nu} &= 10, 6 \left( \frac{Sc_t}{Sc} \right)^{0.26} \\ k_{lim} &= \frac{J_{lim}}{zFC_\infty u_\tau} = 0.10 Sc^{-0.74} Sc_t^{-0.26} \end{aligned} \right\} \quad (4)$$

$J_{lim}$  depends only on the initial concentration,  $C_\infty$ , on the nature and the temperature of the solution through the Schmidt number,  $Sc$ , and on the friction velocity,  $u_\tau = \sqrt{(\nu|dU/dy|_{y=0})}$ .

It is therefore possible to transpose the results from one cell to another by way of the similarity parameters appearing in Equations 4. The coefficient  $k_{lim} = J_{lim}/zFC_\infty$  for the mass transfer, which represents the ion transport velocity, must be non-dimensionalized using the cathode friction velocity,  $u_\tau$ .

The results obtained for  $k_{lim}$  show that a characteristic length of the cell, like the hydraulic diameter which is generally used, is not an appropriate reference for defining the Sherwood number,  $Sh$ . Electrodeposition is a surface phenomenon that must be evaluated with local quantities. Since the thickness,  $\delta_l$ , of the viscous film limits the growth of the diffusion film, this length, which is of the order of  $5\nu/u_\tau$ , was retained as a characteristic parameter. The Sherwood number then takes the form

$$Sh = \frac{10^{-3} J_{lim} \delta_l}{zFC_\infty D} = 5 \times 10^{-4} \left( \frac{Sc}{Sc_t} \right)^{0.26} \quad (5)$$

which makes it independent of the cell geometry.

The length needed by the film to become established is given by

$$\frac{x_0 u_\tau}{\nu} = 284 Sc_t^{0.78} Sc^{0.22}$$

for a Poiseuille flow, and by

$$\frac{x_0 u_\tau}{\nu} = 56 \frac{V_b}{u_\tau} Sc_t^{0.52} Sc^{0.48}$$

for a Couette–Poiseuille flow.

Application of these laws to typical geometries shows that laboratory facilities should be designed with the greatest electrode area possible, in order to ensure that the establishment length be small compared to the length of the electrode. As an example, the establishment length,  $x_0$ , represents 5% of a 125 mm electrode for standard working conditions. In an industrial cell, the length  $x_0$ , which depends on the cathode displacement velocity  $V_b$ , is always small compared to the electrode length.

Equation 5 shows that the Sherwood number varies with the molecular Schmidt number to a power of about 1/4, which is in agreement neither with the Chilton–Colburn [7] nor with the Vielstich [8] models, in which this power is 1/3. The present results are more in agreement with those of Deissler [9], who obtained a power of 0.25. Ibl [5] has already addressed the question of the value of this exponent and emphasized that most of the laws are derived from analogies with heat transfer, for which the molecular Schmidt number is close to unity. This author pointed out that in electrochemistry this Schmidt number is a hundred to a thousand times higher. In this case a variation at a power of 0.25 should be more likely. The numerical results presented here support this analysis.

### 3. Experimental study

To validate the calculations and to determine the value of the turbulent Schmidt number  $Sc_t$ , experiments were performed in a laboratory cell (Fig. 4) using electrodes of 2 dm<sup>2</sup> area (160 mm wide by 125 mm long). A cell with a large electrode area was chosen, in order to limit the effects of edges and of the establishment of the concentration profile. The cross section of the channel was rectangular. The distance between the electrodes is 5 mm and the channel width was the same as that of the electrodes, i.e. 160 mm. The channel was 600 mm long upstream of the electrodes. This is a sufficient length to be sure that the flow is established prior to the electrodes. The channel was equipped with a longitudinal and transverse lattice of static pressure taps to verify the flow quality and uniformity (over the width of the electrodes). The pressure measurements were also used to control the establishment of the flow and as a validation of an electromagnetic flowmeter.

The electrolyte used was an acid solution of zinc sulphate ( $[H_2SO_4] = 0.87 \text{ M}$ ,  $[ZnSO_4] = 1 \text{ M}$ ). This solution was pumped from a 100 dm<sup>3</sup> tank. With this volume of electrolyte, a large number of tests were run with no noticeable variation of zinc concentration. The tank temperature was regulated using an immersed radiator controlled by a platinum temperature probe. For the present study it was fixed

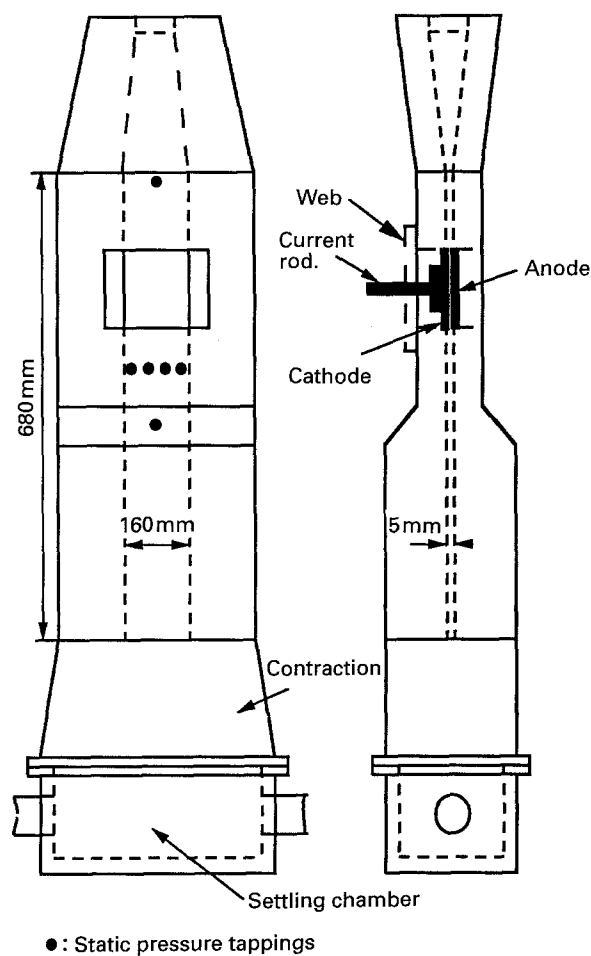


Fig. 4. Experimental setup. Flow velocity can be varied from 0 to 5 m s<sup>-1</sup>, current density from 0 to 300 A dm<sup>-2</sup>.

at 50°C. The mean velocity in the cell was adjusted by use of a bypass, and was varied from 0 to 5 m s<sup>-1</sup>.

The electrolysis current was supplied from a rectifier generating a current density up to 300 A dm<sup>-2</sup>. An integrator coupled to the anemometer gave the quantity of electricity used (in C).

The cathode surface was degreased and electrochemically brightened. It was verified that the surface roughness of the electrodes had no noticeable influence on the flow or on the current density measurement. Two cathode roughnesses were tested: they correspond to relative roughnesses  $Ra = 0.7$  and 1.8. The results are identical for both.

The measurement method used was the codeposition of a tracer described by Degrez and Winand [10]. The tracer used was cadmium. To ensure that the cadmium deposited at its limited current density, its concentration was varied over a large range. A cadmium concentration of about 1 mol m<sup>-3</sup> (that is a thousand times less than that of zinc) was retained.

In zinc electrodeposition, the cathode efficiency is not 100%. The hydrogen released at the cathode greatly affects the diffusion limited current density, and thus the deposit. To determine the cathode efficiency with the greatest possible precision, the total weight of the electrode was measured, before and after electrolysis, on a balance with a precision

of  $10^{-2}$  g. The difference, being the weight of the deposit which is of the order of 1.5 g, was compared to the coulombic measurement by the integrator to determine the cathode efficiency.

More than 250 experiments were performed using a series of 15 plates. In each series, five different conditions were tested three times each in order to validate the results. The flow velocity was varied from 0 to  $5 \text{ m s}^{-1}$ . The current density was also varied from 50 to  $150 \text{ A dm}^{-2}$  to study the effect of the quantity of hydrogen released. The current efficiencies obtained varied very little, from 92 to 97%.

The hydrogen released at the cathode locally disturbs the flow and makes it more turbulent: consequently, the measurements do not correspond to the numerical simulations. Figure 5 shows the values of  $k_{\text{lim}}/u_\tau$  obtained experimentally and numerically, as a function of the Reynolds number  $Re = U_q h/\nu$  ( $U_q$  being the mean flow velocity). It can be seen that the differences between the measured and computed values are large at low Reynolds numbers, but that the experimental data tend asymptotically toward the numerical solution as the flow velocity and, consequently, the Reynolds number increases. This result may be interpreted as follows: as the Reynolds number increases, the hydrogen bubbles are removed from the cathode surface more rapidly. The influence of the hydrogen on the flow can thus be interpreted by considering that it generates additional agitation in the vicinity of the cathode [6, 11–13]. In fact, the results obtained here have shown that  $J_{\text{lim}}$  increases according to the same law, whether the flow velocity or the quantity of gas emitted is increased. The additional agitation due to the gas can thus be modelled by a hypothetical friction velocity, denoted  $u_\tau^*$ , which is higher than  $u_\tau$  and which depends on the amount of hydrogen released. From the analysis of the experimental results, it may be proposed that this friction velocity  $u_\tau^*$  is the sum of the friction velocity  $u_\tau$  of the flow considered without bubbles and of a term which is proportional to the quantity of gas

emitted per unit time:

$$u_\tau^* = u_\tau \left[ 1 + 25\,000 \left( \frac{100 - \eta}{100} \right) \frac{k}{u_\tau} \right] \tag{6}$$

where  $\eta$  is the cathode efficiency and  $k$  the mass transfer coefficient obtained at the working current density.

Taking this correction into account, the comparison of the measurements with the model Equation 4 gives the turbulent Schmidt number: i.e.  $Sc_t = 1.14$ . This value is close to unity, as assumed by the theory [3]. It is then possible to propose a model that takes into account the effect of the flow, of the solution composition and temperature and of the presence of hydrogen, on the diffusion limited current density.

$$\frac{k_{\text{lim}}}{u_\tau^*} = 0.1 Sc^{-0.74} Sc_t^{-0.26} \tag{7}$$

In Fig. 6 the predictions of the proposed model are compared with the experimental results obtained in the present study for different flow conditions and different current densities. The measurements are in good agreement with the predictions. As the composition and the temperature of the solution are fixed ( $Sc$  constant),  $k_{\text{lim}}/u_\tau^*$  is constant for any  $k$  or  $u_\tau$ . The application of Equation 7 to the experiments described by Wang *et al.* [6] is presented in Fig. 7, where  $Re_q$  is the Reynolds number based on the flow velocity and the hydraulic diameter. For these experiments the solution temperature and composition were constant. By using the friction velocity  $u_\tau^*$ , the ratio  $k_{\text{lim}}/u_\tau^*$  becomes independent of the Reynolds number, whether hydrogen is released or not; but the measurements differ greatly, in level, from the model. These differences can be explained as follows:

(i) Picket and Ong [7] have studied the effect of electrode dimensions on the measurements. On an electrode of 20 mm in length, they measured a mass transfer coefficient which was 70% greater than on a 150 mm electrode. The electrodes used by Wang *et al.* [6] are of small dimensions.

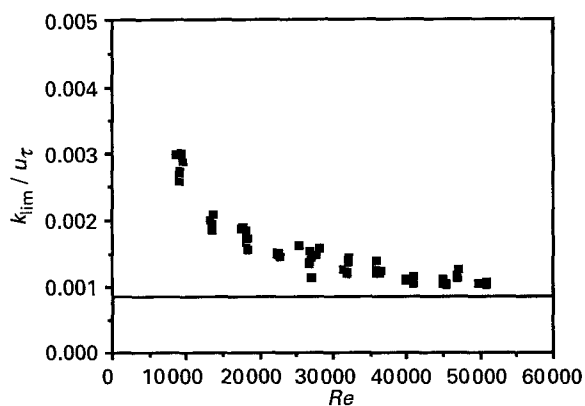


Fig. 5. Comparison between the measurements obtained in the cell of Fig. 4 (■) and Equation 5 (—) resulting from the numerical modelling for the limiting mass transfer coefficient as a function of the Reynolds number. The influence of hydrogen production decreases with increasing Reynolds number.

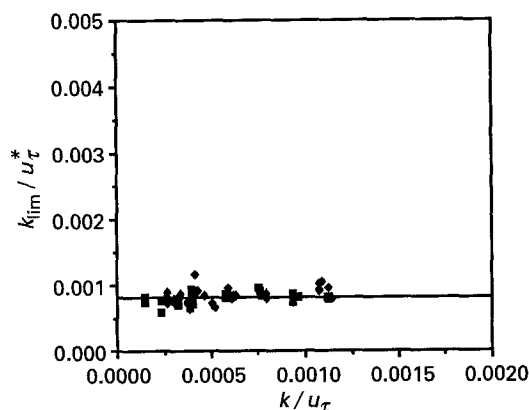


Fig. 6. Comparison of the law of Equation 8 (—) with the experimental results obtained for constant flow conditions (■) and a constant current density (◆). The influence of hydrogen production has been corrected by using a fictitious friction velocity  $u_\tau^*$ .

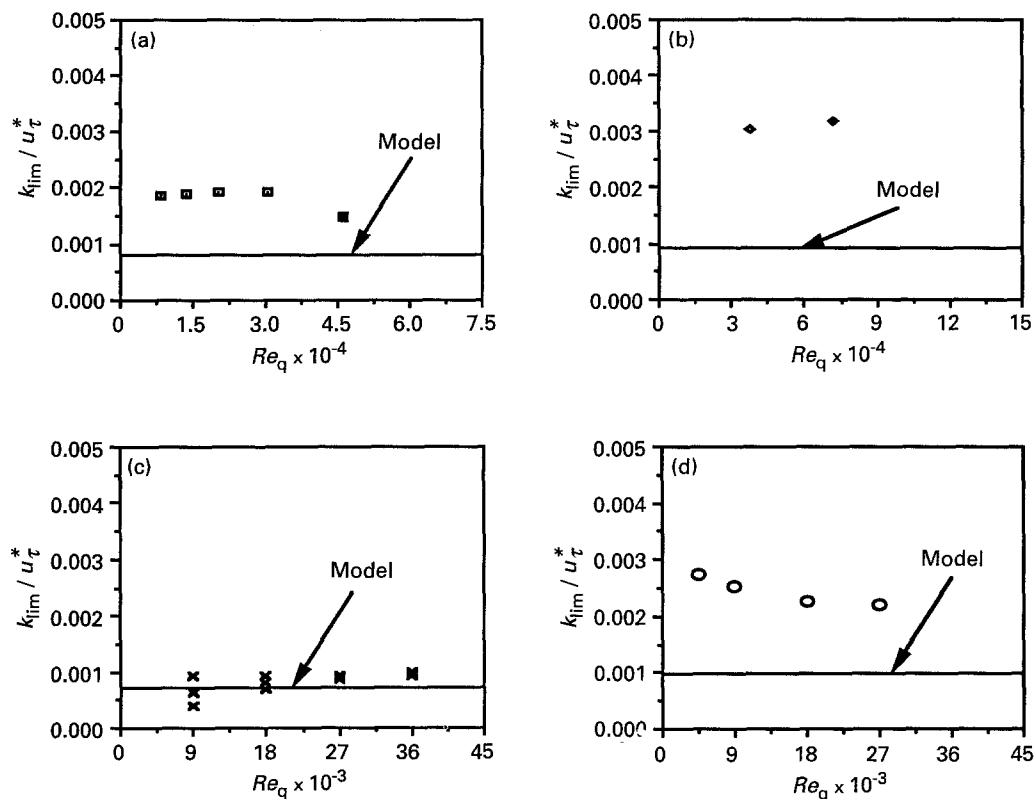


Fig. 7. Application of the full model of Equation 8 (—) to the experimental results of [6]. The influence of hydrogen production is corrected by the proposed model. The difference in level is attributed to the difference in electrode size and cell geometry. Sources: (a) [6, Table 2]; (b) [6, Table 3]; (c) [6, Table 5] and (d) [6, Table 6]. The following tabulated information is applicable.

Fig.	Metal	Tracer	Channel section/mm <sup>2</sup>	Remarks
(a)	copper	silver	□ 16 × 15	no hydrogen
			■ 18 × 6	
(b)	copper	silver	200 × 15	no hydrogen
(c)	zinc	cadmium	18 × 6	hydrogen generation
(d)	zinc	—	18 × 6	measured by potentiodynamic method

(ii) Picket and Ong [7] have also shown that if the flow is not perfectly established before it reaches the electrode, an apparent increase in the measured mass transfer coefficient is observed. This precaution was taken in our experiments.

(iii) The cells used by Wang *et al.* [6] have rectangular cross sections with an aspect ratio that is not sufficiently high. The friction velocity used in Equation 7 was then the average around the perimeter of the channel, determined from the head loss coefficient (Blasius law). This friction velocity does not correspond to that on the electrode itself.

#### 4. Conclusions

To characterize the diffusion film that develops along a moving or stationary cathode, an investigation has been performed by way of a numerical simulation using simple turbulence models. The results show that, in a turbulent flow, the thickness of the diffusion film is close to that of the viscous sublayer. This viscous sublayer thickness and the surface friction

velocity are therefore chosen as characteristic quantities. A model relating the Sherwood number to the molecular and turbulent Schmidt numbers has been proposed. This model does not depend on the cell geometry. It differs from that proposed by Chilton–Colburn [7] and agrees well with that of Deissler [9], which is more realistic considering the order of magnitude of the molecular Schmidt number. An experimental study, in the case of zinc electrodeposition, validates the proposed model. It allows a friction velocity correction that takes the release of hydrogen correctly into account. It also shows that the turbulent Schmidt number is of order unity.

From the present study, it appears that the results obtained in a laboratory cell can be transposed to an industrial cell by verifying the constancy of the similarity parameters appearing in Equations 5 and 6. The diffusion limited current density, which determines the texture of the deposit, can then be deduced from Equation 8. The flow influence appears through the friction velocity  $u_\tau$  along the cathode. The molecular Schmidt number enters to a 1/4 power.

Hydrogen release can be introduced to the equation by assuming that the disturbance it creates in the flow corresponds to an increased agitation, which can be represented by a fictitious friction velocity  $u_{\tau}^*$ .

From the results of the present study and by comparison with other existing results, it can also be shown that the electrode area of a laboratory cell must be large enough to make the edge effects negligible.

The model proposed in Equation 8 remains to be confirmed, mainly by electrode-position tests without release of hydrogen, e.g. with copper, and by a more detailed analysis of the effect of the gaseous release at the cathode on the diffusion limited current density.

### References

- [1] R. Winand, 'High current density electrocrystallization'. Proc. Int. Conf. on Zinc and Zinc Alloy Coated Steel Sheet (GALVAT-ECH), Tokyo, The Iron and Steel Institute of Japan (1989).
- [2] J. C. Monnier, 'Hydrodynamique des écoulements turbulents dans les cellules d'électro-déposition'. Thèse de doctorat, UST Lille Flandres Artois (1989).
- [3] J. Newman, 'Electrochemical systems', Prentice-Hall, New York (1973).
- [4] L. Vanhee, 'Contribution à l'étude du comportement hydrodynamique des cellules d'électro-déposition'. Thèse de doctorat, UST Lille Flandres Artois (1991).
- [5] N. Ibl, *Electrochim. Acta* **22** (1977) 465.
- [6] H. M. Wang, S. F. Chen, T. J. O'Keefe, M. Degrez and R. Winand, *J. Appl. Electrochem.* **19** (1989) 174.
- [7] D. J. Pickett and K. L. Ong, *Electrochim. Acta* **19** (1974) 875.
- [8] A. Weymeersch, R. Winand and L. Renard, *Plat. Surf. Finish.* **68** (1981) 56; **68** (1981) 118.
- [9] R. G. Deissler, 'Analysis of turbulent heat transfer and flow in the entrance regions of smooth passages'. Committee for Aeronautics, Report 3016 (1953).
- [10] M. Degrez and R. Winand, 'Contribution à la mise au point de la méthode de mesure des densités de courant limite de diffusion par co-déposition d'un traceur. Cas particulier du cuivre'. *Revue ATB Met.* **XIX** (1/2) (1979) 21.
- [11] F. A. Rodriguez, M. Degrez and R. Winand, *Oberfläche Surface* **30**(8) (1989) 20.
- [12] M. Degrez, F. A. Rodriguez and R. Winand, *Oberfläche Surface* **30**(9) (1989) 14.
- [13] R. Winand, *J. Appl. Electrochem.* **21**, (1991) 377.